Hindawi Publishing Corporation
Mathematical Problems in Engineering
Volume 2014, Article ID 658093, 9 pages
http://dx.doi.org/10.1155/2014/658093

Research Article

A Pan-Function Model for the Utilization of Bandwidth Improvement and PAPR Reduction

Yidong Xu, Wei Xue, and Wenjing Shang

College of Information and Communication Engineering, Harbin Engineering University, Harbin 150001, China

Correspondence should be addressed to Wei Xue; xuewei@hrbeu.edu.cn

Received 7 June 2014; Revised 4 September 2014; Accepted 18 September 2014; Published 19 October 2014

Academic Editor: Marek Lefik

Aiming at the digital quadrature modulation system, a mathematical Pan-function model of the optimized baseband symbol signals with a symbol length of $4T$ was established in accordance with the minimum out-band energy radiation criterion. The intersymbol interference (ISI), symbol-correlated characteristics, and attenuation factor were introduced to establish the mathematical Pan-function model. The Pan-function was added to the constraints of boundary conditions, energy of a single baseband symbol signal, and constant-envelope conditions. Baseband symbol signals with the optimum efficient spectrum were obtained by introducing Fourier series and minimizing the Pan-function. The characteristics of the spectrum and peak-to-average power ratio (PAPR) of the obtained signals were analyzed and compared with the minimum shift keying (MSK) and quadrature phase-shift keying (QPSK) signals. The obtained signals have the characteristics of a higher spectral roll-off rate, less out-band radiation, and quasi-constant envelope. We simulated the performance of the obtained signals, and the simulation results demonstrate that the method is feasible.

1. Introduction

Modern communications require modulation signal robust to nonlinear channel and adjacent-channel interference (ACI). For example, deep-space communication channel [1, 2] is a typical band-limited and nonlinear variable-parameter channel. Signals are band-limited to avoid the transmitter signals causing interference on the adjacent channel and the band limit to filter a part of the energy outside the frequency spectrum, which may distort the filtered signals. The envelope fluctuation signals passing through nonlinear processing components can cause amplitude-to-phase modulation (AM/PM) effects, causing phase noise and spectral spreading. Therefore, the nonlinear channel characteristics make higher demands on the input signals. Traditional digital modulations have been unable to meet the requirements of the application, and a new digital modulation scheme need to be adopted to reduce the channel impact on signals, thus achieving higher transmission rates under limited bandwidth [3–6]. To better solve this problem, the demand for modulation techniques with higher standards has increased in recent years. Thus, the criterion requirements set by the U.S. Federal Communications Commission (FCC) for visual range wireless relay communication systems include the following: (1) 99% of the signal power included in the occupied bandwidth, (2) out-band radiation <1%, (3) the frequency-band utilization rate equal to or >1 bit/s/Hz, and (4) constant or quasi-constant envelope. Based on these requirements, many constant-envelope modulation techniques with high bandwidth efficiency rather than multilevel amplitude modulations have been developed, such as offset QPSK (OQPSK) [7], MSK [8, 9], Gaussian minimum shift keying (GMSK) [10, 11], and filtered QPSK (FQPSK) [12]. So far, new digital modulation techniques are being developed.

This study aimed to achieve one of the optimized spectrum signals based on the digital communication system requirements, with characteristics of a higher spectral roll-off rate, less out-band radiation, and quasi-constant envelope.

2. Foundation of the Optimized Mathematical Model

2.1. Minimum Energy Radiation Criterion outside the Frequency Bands. To obtain the quadrature-modulated baseband symbol signals with the characteristics of a higher

spectral roll-off rate, the minimum out-band radiation criterion involved [13] can be expressed as follows:

$$J = \frac{1}{2\pi}\int_{-\infty}^{+\infty} g(\omega)\,|S(\omega)|^2 d\omega, \tag{1}$$

where the Fourier transform of $a(t)$ is

$$S(\omega) = \int_{-T/2}^{T/2} a(t)\, e^{-j\omega t} dt. \tag{2}$$

$a(t)$ is the symbol signal waveform, which is an even function assumed in interval $[-T/2, T/2]$, T is the symbol period, $|S(\omega)|^2$ is the power spectrum of $a(t)$, and $g(\omega)$ is the increasing function that determines the roll-off rate of the spectral density function $S(\omega)$. The increasing function $g(\omega) = \omega^{2n}$ $(\omega > 0)$ with different n values is shown in Figure 1. The value of n depends on the degree of suppressed out-band radiation. To make the functional integral J convergent and integrable, the roll-off rate of $|S(\omega)|^2$ should be greater than the increase rate of $g(\omega)$ to limit the roll-off rate of the power spectrum $|S(\omega)|^2$ of the signal $a(t)$.

The power spectral density of $a(t)$ can be written as follows:

$$|S(\omega)|^2 = \iint_{-T/2}^{T/2} a(t)\, a(s)\, e^{-j\omega(t-s)} dt\, ds. \tag{3}$$

Replacing (3) into (1), and after some manipulations, we obtain the following:

$$J = \frac{1}{2\pi}\int_{-\infty}^{+\infty}\iint_{-T/2}^{T/2} g(\omega)\, a(t)\, a(s)\, e^{-j\omega(t-s)} dt\, ds\, d\omega. \tag{4}$$

To facilitate the solution, the function $g(\omega)$ can be expressed as follows:

$$g(\omega) = \lim_{r\to 0} g(\omega)\, e^{-r\omega} = \lim_{r\to 0} \omega^{2n} e^{-r\omega} \quad (r \geq 0). \tag{5}$$

When r lies on interval $[0, +\infty]$, the integral $\int_{-\infty}^{+\infty} \omega^{2n} e^{-r\omega} e^{-j\omega(t-s)} d\omega$ is convergent; therefore, the order of the integral can be exchanged as follows:

$$J = \frac{1}{2\pi}\lim_{r\to 0}\iint_{-T/2}^{T/2} a(t)\, a(s)\left[\int_{-\infty}^{+\infty} \omega^{2n} e^{-r\omega} e^{-j\omega(t-s)} d\omega\right] dt\, ds. \tag{6}$$

Based on the Taylor series expansion,

$$e^{-r\omega} = 1 - r\omega + \left(\frac{r\omega}{2!}\right)^2 + \cdots + \frac{(-r\omega)!}{n!} + \cdots \tag{7}$$

According to Fourier inverse transform [14], $\delta(t)$ can be written as follows:

$$\delta(t) = \frac{1}{2\pi}\int_{-\infty}^{+\infty} e^{j\omega t} d\omega. \tag{8}$$

Because $\delta(t)$ is an even function,

$$\delta(t) = \frac{1}{2\pi}\int_{-\infty}^{+\infty} e^{-j\omega t} d\omega, \tag{9}$$

$$\delta(t-s) = \frac{1}{2\pi}\int_{-\infty}^{+\infty} e^{-j\omega(t-s)} d\omega. \tag{10}$$

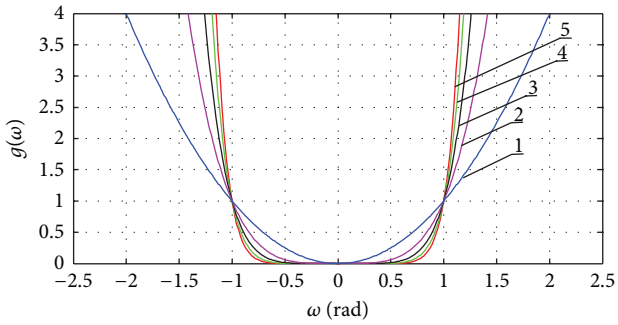

Figure 1: Waveforms of $g(\omega)$ under different values of n.

Hence, the following equation can be obtained:

$$\frac{\partial^{2n}(\delta(t-s))}{\partial t^{2n}} = \delta^{(2n)}(t-s) = \frac{(-j)^{2n}}{2\pi}\int_{-\infty}^{+\infty} \omega^{2n} e^{-j\omega(t-s)} d\omega. \tag{11}$$

When $r \to 0^+$ and replacing (10) and (11) into (6), the following expression can be obtained:

$$\begin{aligned} J &= \iint_{-T/2}^{T/2} a(t)\, a(s)\,(-1)^n \delta^{(2n)}(t-s)\, dt\, ds \\ &= (-1)^n \int_{-T/2}^{T/2} a(t)\left[\int_{-T/2}^{T/2} \delta^{(2n)}(t-s)\, a(s)\, ds\right] dt. \end{aligned} \tag{12}$$

Using the characteristics of $\delta(t)$ function, (12) can be written as follows:

$$J = (-1)^n \int_{-T/2}^{T/2} a(t)\, a^{(2n)}(t)\, dt, \tag{13}$$

where $a^{(2n)}(t)$ is the $2n$-order derivative of the symbol signal.

According to (13), the criterion for minimum out-band radiation can be transformed into the problem of unraveling the symbol function $a(t)$ when minimizing the Pan-functional J [15].

In general, for serial-to-parallel (S/P) converter in quadrature modulation system, the parallel symbol duration is $2T$ twice of the input symbol duration in in-phase and orthogonal channels without intersymbol interference. Based on Nyquist's second criterion, by introducing controlled intersymbol interference on the sampling time of some symbols, the requirement of timing accuracy can be reduced, while the remaining symbols without intersymbol interference on the sampling time utilize theoretical maximum bandwidth.

By allowing a controlled amount of intersymbol interference, the partial-response signals could be achieved with a symbol transmission rate of $1/T$ [16]. The symbol duration increased to $4T$, while the length of intersymbol interference was $2T$. According to the theory of the relationships between frequency and time domains, when the length of the signal in time domain increased, the spectrum became narrow in frequency domain indicating that a higher spectral roll-off rate was obtained. The baseband signals were obtained with

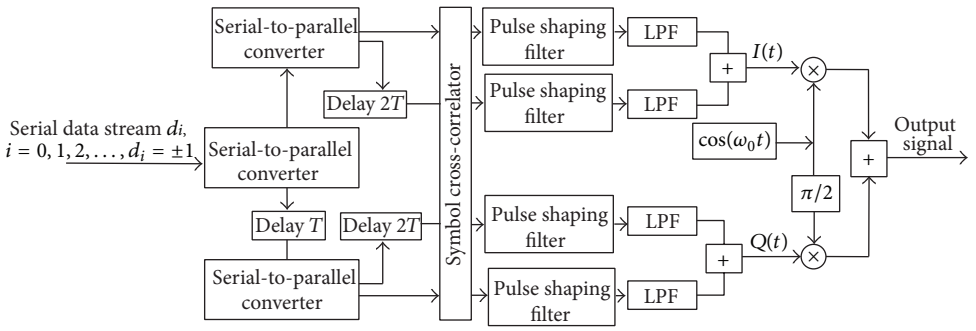

Figure 2: Block diagram of the quadrature modulation system.

good spectrum characteristics, fulfilling the purpose of introducing controlled intersymbol interference. Furthermore, this intersymbol interference slightly affected the correct receiving and decision of signals. Clearly, if the symbol duration is increased to $4T$, then (11) can be expressed as follows:

$$J = (-1)^n \int_{-2T}^{2T} a(t)\, a^{(2n)}(t)\, dt. \tag{14}$$

2.2. Additional Constraints of Pan-Function. The block diagram of the adopted quadrature modulation system with intersymbol interference and symbol-correlated characteristics is shown in Figure 2. This can be interpreted as the cascade of the following.

(1) Three S/P converters group the symbols d_i, $i = 0, 1, 2, \ldots$, with a symbol duration of T into four blocks, each taking one of the values ± 1, where the delay time is a different integer multiple of T and the symbol duration is increased to $4T$.

(2) According to the results of the symbol cross-correlation operation, symbol cross-correlator and attenuation factor r were introduced, and r lies on interval $(0, 1]$.

(3) The output signal from pulse shaping filter was low-pass filtered, yielding signals $I(t)$ and $Q(t)$ in two channels.

(4) The signals, $I(t)$ and $Q(t)$, were multiplied to the quadrature carrier and added to obtain the modulated signal as follows:

$$S(t) = I(t)\cos(\omega t) + Q(t)\sin(\omega t), \tag{15}$$

where

$$I(t) = \sum_{n=-N}^{N} d_{2n-1} r_{2n-1} a[t - (2n-1)T] + d_{2n+1} r_{2n+1} a[t - (2n+1)T],$$

$$Q(t) = \sum_{n=-N}^{N} d_{2n} r_{2n} a(t - 2nT) + d_{2n+2} r_{2n+2} a[t - (2n+2)T]. \tag{16}$$

Herein, four signal channels were introduced to not to overlap the time of each channel adjacent to baseband symbol signal, because the optimal time length of the symbol signal is $4T$.

Then, the mathematical Pan-function (14) was added to the constraints of boundary conditions, energy of a single-symbol signal, and constant-envelope conditions.

2.2.1. Restriction on the Symbol Boundary Condition. From [17], assuming that function $a(t)$ is in the finite interval $[-T/2, T/2]$, if $a(t)$, $a'(t)$, $a''(t), \ldots, a^{(n-1)}(t)$ are continuous in interval $[-T/2, T/2]$ without skipping, and $a^{(n)}(t)$ is finite, then there is no skipping in the end point of the interval; that is, $a(\pm T/2) = a'(\pm T/2) = \cdots = a^{(n-1)}(\pm T/2) = 0$. The Fourier transform of $a(t)$ decays not less than C/ω^{n+1} in the finite interval $[-T/2, T/2]$, where C is a constant.

Herein, assuming that $a(t)$ is an even function on interval $[-2T, 2T]$, $a(t)$ should satisfy the following boundary condition:

$$a(\pm 2T) = a(\pm 2T)' = \cdots = a^{(n-1)}(\pm 2T) = 0. \tag{17}$$

2.2.2. Restriction on the Single-Symbol Signal Energy Condition. For the signal $a(t)$ with a length of $4T$, the energy per transmission can be expressed as follows:

$$E = \int_{-2T}^{2T} a^2(t)\, dt. \tag{18}$$

2.2.3. Restriction on the Constant-Envelope Condition of the Quadrature-Modulated Signal. The constant-envelope modulation means that the envelope of modulated wave should be constant, the generated modulation signal is band-limited by the transmitter, and only a small spectrum spreading is produced after the signal passes through the nonlinear processing components. The envelope fluctuation of the signal is measured by the PAPR of modulation signals; when the PAPR of the signal is equal to or close to 1 [18, 19], constant-envelope modulation can be achieved.

In the quadrature modulation system, to achieve a constant envelope, the ratio of the output signal peak power to the

average power should be made close to 1. Thus, the following conditions should be satisfied when t lies on interval $[0, 4T]$:

$$I^2(t) + Q^2(t) = \text{const.} \tag{19}$$

According to the symmetry of the signal, we only need to consider whether (19) can be satisfied when t lies on interval $[0, 2T]$ at any time; then, the condition will be satisfied on other intervals. The baseband signal of $I(t)$ and $Q(t)$ on interval $[0, 2T]$ can be expressed as follows:

$$\begin{aligned} I(t) &= r_{-1}d_{-1}a(t+T) + r_1 d_1 a(t-T) + r_3 d_3 a(t-3T), \\ Q(t) &= r_0 d_0 a(t+T) + r_2 d_2 a(t-2T), \end{aligned} \tag{20}$$

where d_{-1}, d_0, d_1, d_2, d_3 are the uncorrelated binary data symbols, each taking one of the values ± 1. In (20), attenuation factor r_k was introduced according to the results of the symbol cross-correlation operation, and r_k takes the value 1 or specific r. The five symbols on the interval are $a(t+T)$, $a(t)$, $a(t-T)$, $a(t-2T)$, and $a(t-3T)$. The analysis indicates that if the condition of constant envelope can be satisfied when t lies on interval $[0, T]$, then in the other intervals, this condition can still be satisfied. In this case, the four symbols on the interval are, respectively, d_{-1}, d_0, d_1, d_2. In this manner, we can greatly simplify the calculation process. The different conditions are as follows.

(1) When $d_{-1} \cdot d_1 = 1$, the adjacent baseband symbol signals have the same sign in the I channel.

(a) When $d_0 \cdot d_2 = 1$, the adjacent baseband symbol signals have the same sign in the Q channel, and to meet the constant-envelope condition, we should introduce the attenuation factor r on $[0, 1]$. In this case

$$\begin{aligned} I_{11}^2(t) &= r^2 a^2(t-T) + a^2(t+T) \\ &\quad + 2ra(t+T)\,a(t-T), \\ Q_{21}^2(t) &= r^2 a^2(t) + a^2(t-2T) \\ &\quad + 2ra(t)\,a(t-2T). \end{aligned} \tag{21}$$

(b) When $d_0 \cdot d_2 = -1$, the adjacent baseband symbol signals have the opposite sign in the Q channel, and to satisfy (19)

$$\begin{aligned} I_{12}^2(t) &= a^2(t-T) + a^2(t+T) \\ &\quad + 2a(t+T)\,a(t-T), \\ Q_{22}^2(t) &= r^2 a^2(t) + a^2(t-2T) \\ &\quad - 2ra(t)\,a(t-2T). \end{aligned} \tag{22}$$

Herein, the value of constant envelope was set to be $a(0)$, which is the value of $a(t)$ at time $t = 0$. Assuming that $a(0)$ is the maximum value of signal $a(t)$, this set is reasonable. To ensure that the modulated signal always has a constant envelope in interval $[0, T]$, the constant-envelope condition is rewritten as follows:

$$\begin{aligned} &\int_0^T \left(I_{11}^2(t) + Q_{21}^2(t) - a^2(0)\right)^2 dt = 0, \\ &\int_0^T \left(I_{12}^2(t) + Q_{22}^2(t) - a^2(0)\right)^2 dt = 0. \end{aligned} \tag{23}$$

(2) When $d_{-1} \cdot d_1 = -1$, the adjacent baseband symbol signals have the opposite sign in the I channel.

(a) When $d_0 \cdot d_2 = 1$, the adjacent baseband symbol signals have the same sign in the Q channel, and to satisfy (19)

$$\begin{aligned} I_{13}^2(t) &= r^2 a^2(t-T) + a^2(t+T) \\ &\quad - 2ra(t+T)\,a(t-T), \\ Q_{23}^2(t) &= a^2(t) + a^2(t-2T) \\ &\quad + 2a(t)\,a(t-2T). \end{aligned} \tag{24}$$

(b) When $d_0 \cdot d_2 = -1$, the adjacent baseband symbol signals have the opposite sign in the Q channel, and to satisfy (19)

$$\begin{aligned} I_{14}^2(t) &= a^2(t-T) + a^2(t+T) \\ &\quad - 2a(t+T)\,a(t-T), \\ Q_{24}^2(t) &= a^2(t) + a^2(t-2T) \\ &\quad - 2a(t)\,a(t-2T). \end{aligned} \tag{25}$$

Similar to (23), when $d_{-1} \cdot d_1 = -1$, the constant-envelope condition can be expressed as follows:

$$\begin{aligned} &\int_0^T \left(I_{13}^2(t) + Q_{23}^2(t) - a^2(0)\right)^2 dt = 0, \\ &\int_0^T \left(I_{14}^2(t) + Q_{24}^2(t) - a^2(0)\right)^2 dt = 0. \end{aligned} \tag{26}$$

Based on the comprehensive consideration of formulas (23) and (26) and various combinations of random data symbols in interval $[0, T]$, to decrease the number of constants in the Pan-function, the constant-envelope condition can be expressed by an integral formula as follows:

$$\begin{aligned} \int_0^T \Big(&\left(I_{11}^2(t) + Q_{21}^2(t) - a^2(0)\right)^2 \\ &+ \left(I_{12}^2(t) + Q_{22}^2(t) - a^2(0)\right)^2 \\ &+ \left(I_{13}^2(t) + Q_{23}^2(t) - a^2(0)\right)^2 \\ &+ \left(I_{14}^2(t) + Q_{24}^2(t) - a^2(0)\right)^2 \Big) dt = 0. \end{aligned} \tag{27}$$

Thus, in the Pan-function with the constraints of single-symbol energy and quadrature modulation signals, the constant-envelope conditions can be expressed as follows:

$$\begin{aligned} H = J &+ \lambda\left(\int_{-2T}^{2T} a^2(t)\,dt - E\right) \\ &+ \mu\int_0^T \left(\left(I_{11}^2(t) + Q_{21}^2(t) - a^2(0)\right)^2\right. \\ &\quad + \left(I_{12}^2(t) + Q_{22}^2(t) - a^2(0)\right)^2 \\ &\quad + \left(I_{13}^2(t) + Q_{23}^2(t) - a^2(0)\right)^2 \\ &\quad \left. + \left(I_{14}^2(t) + Q_{24}^2(t) - a^2(0)\right)^2\right) dt, \end{aligned} \tag{28}$$

where λ and μ are the Lagrange constants.

3. Solution Process of the Optimized Signal

3.1. Signal Solving Process Using Fourier Series. Any function in interval $[-2T, 2T]$ can be infinitely approximated by Fourier series [20]. The efficient spectrum signal $a(t)$, with a code width of $4T$, can be expressed in the following Fourier series form:

$$a(t) = \frac{a_0}{2} + \sum_{k=1}^{m}\left(a_k\cos\left(\frac{\pi}{2T}kt\right) + b_k\sin\left(\frac{\pi}{2T}kt\right)\right), \tag{29}$$

where

$$\begin{aligned} a_0 &= \frac{1}{2T}\int_{-2T}^{2T} a(t)\,dt, \\ a_k &= \frac{1}{2T}\int_{-2T}^{2T} a(t)\cos\left(\frac{\pi}{2T}kt\right)dt, \\ b_k &= \frac{a_0}{2} + \sum_{k=1}^{m} a_k\cos\left(\frac{\pi}{2T}kt\right). \end{aligned} \tag{30}$$

$a(t)$ was set as an even function; therefore, $b_k = 0$, and $a(t)$ can be expressed as follows:

$$a(t) = \frac{a_0}{2} + \sum_{k=1}^{m} a_k\cos\left(\frac{\pi}{2T}kt\right). \tag{31}$$

Replacing (31) into (14), J can be expressed compactly as follows:

$$J = 2T\sum_{k=1}^{m} a_k^2\left(\frac{\pi}{2T}k\right)^{2n}. \tag{32}$$

Introducing energy restriction into (31), the following expression can be obtained:

$$\frac{E}{2T} - \left(2\sum_{k=1}^{m}(-1)^{k+1}a_k\right)^2 - \sum_{k=1}^{m} a_k^2 = 0. \tag{33}$$

Table 1: Coefficient of Fourier series and signal PAPR.

n	m	r	a_0	a_1	a_2	a_3	PAPR
3	3	0.8	0.736	0.469	0.089	−0.01	1.04
		0.9	0.709	0.480	0.130	0.004	1.05
		1.0	0.692	0.484	0.152	0.013	1.07

Using (32) and (33), (28) can be written as follows:

$$\begin{aligned} H = &2T\sum_{k=1}^{m} a_k^2\left(\frac{\pi}{2T}k\right)^{2n} \\ &+ \lambda\left(\frac{E}{2T} - \left(2\sum_{k=1}^{m}(-1)^{k+1}a_k\right) - \sum_{k=1}^{m} a_k^2\right)^2 \\ &+ \mu\int_0^T \left(\left(I_{11}^2(t) + Q_{21}^2(t) - a^2(0)\right)^2\right. \\ &\quad + \left(I_{12}^2(t) + Q_{22}^2(t) - a^2(0)\right)^2 \\ &\quad + \left(I_{13}^2(t) + Q_{23}^2(t) - a^2(0)\right)^2 \\ &\quad \left. + \left(I_{14}^2(t) + Q_{24}^2(t) - a^2(0)\right)^2\right) dt. \end{aligned} \tag{34}$$

The normalizations, $E = 1$, $T = 1$, and the specific values of r were assumed; only the coefficients, $a_0, a_1, \ldots, a_m$, of the Fourier series and the Lagrange constants, λ and μ, are unknown parameters. Therefore, our goal was to determine the coefficients, $a_0, a_1, \ldots, a_m$, of the Fourier series. Based on the extreme value theory [18] of variational calculus, $a_0, a_1, \ldots, a_m$ that need to be determined should satisfy the following partial differential equations:

$$\begin{aligned} &\frac{\partial H}{\partial a_k} = 0 \quad k = 1, 2, \ldots, m; \\ &\frac{\partial H}{\partial \lambda} = 0; \qquad \frac{\partial H}{\partial \mu} = 0. \end{aligned} \tag{35}$$

The solution of simultaneous equations was used to determine the values of the coefficients, $a_0, a_1, \ldots, a_m$, of the Fourier series and the Lagrange constants, λ and μ.

3.2. Time-Frequency Characteristics of the Optimized Signals. The optimized signals were calculated using the MATLAB software [15]; the results show that selecting the proper number of components in the Fourier series can guarantee the accuracy of the Pan-function solution. Herein, the time-frequency characteristics of the optimized signals were analyzed.

When $n = 3$, $m = 3$ and r is equal to 0.82, 0.94, and 1, respectively; the obtained coefficient of Fourier series and the PAPR of signals are listed in Table 1. The expression of the optimized signal $a(t)$ was obtained by replacing the obtained coefficient of Fourier series into (31). The waveforms of the optimized signals $a(t)$ and their normalized power spectra $G_+(f)/G_+(0)$ are shown in Figures 3 and 4, respectively.

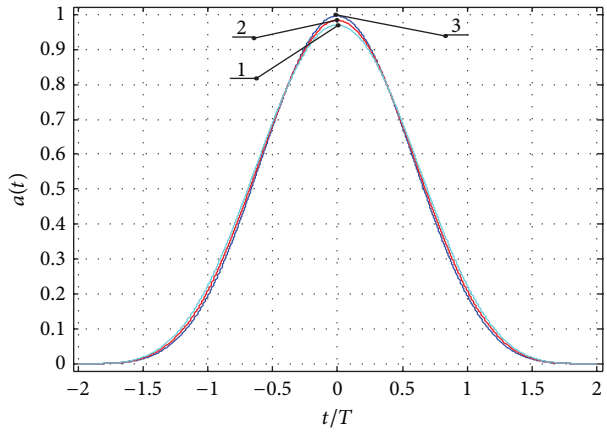

Figure 3: Waveform curves of the optimized signals.

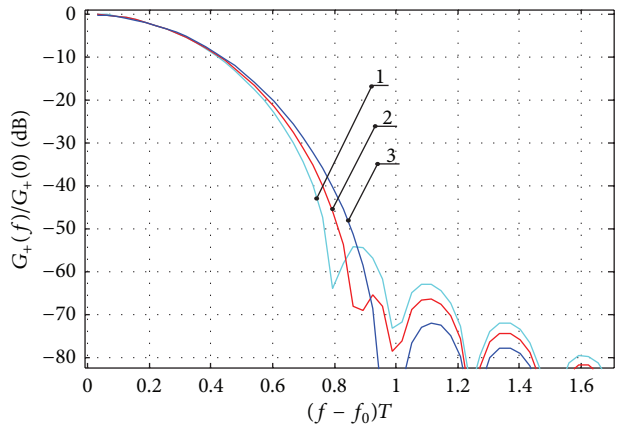

Figure 4: Normalized power spectra curves of the optimized signals.

When $n = 3$, $m = 3$, curves 1–3 in two figures correspond to the waveform of the random sequence signal $a(t)$ and its normalized power spectrum curve, when r is equal to 0.82, 0.94, and 1. Furthermore, the power spectral density of the modulated signal only depends on the power spectrum of a single symbol [20].

Table 2 shows the bandwidth when the normalized power spectra of the optimized signals decrease to −40 dB (ΔF_{-40}) and −60 dB (ΔF_{-60}), the value of the bandwidth containing 90% and 99% of the signal energy ($\Delta F_{90\%}$ and $\Delta F_{99\%}$, resp.), and the PAPR of the optimized signal, under the conditions of different values of n, m, and r.

Figure 2 and Table 2 show the following.

(1) According to the minimum out-band energy radiation criterion, the optimized efficient spectrum signal had a bandwidth of $0.77/T$ (when $n = 3$, $m = 3$, $r = 0.82$, calculated according to −40 dB, namely, ΔF_{-40}) and $0.82/T$ (when $n = 3$, $m = 3$, $r = 0.94$, calculated according to −60 dB, namely, ΔF_{-60}) with the constraints of the baseband signal energy and constant-envelope conditions. Furthermore, the −40 and −60 dB bandwidths decreased by 3.25 and 9.8 times than that of the MSK signal, respectively, while the −40 dB bandwidth decreased by approximately 20.65 times than that of the QPSK signal, thus well inhibiting the signal's out-band energy radiation.

Table 2: Comparison of characteristics of the signals energy spectrum and PAPR.

r	n	m	ΔF_{-40}	ΔF_{-60}	$\Delta F_{90\%}$	$\Delta F_{99\%}$	PAPR
1	1	2	0.88	1.41	0.70	1.04	1.0
		3	0.90	1.42	0.70	1.03	1.0
		4	1.15	1.65	0.76	1.14	1.0
	3	3	0.80	0.90	0.67	1.03	1.0
		4	0.98	1.18	0.67	1.02	1.0
		5	1.39	1.64	0.80	1.22	1.0
	5	4	0.97	1.19	0.68	1.04	1.0
		5	1.29	1.41	0.76	1.13	1.0
		6	1.45	1.59	0.82	1.24	1.0
	7	5	1.41	1.32	0.72	1.08	1.0
		6	1.20	1.41	0.73	1.09	1.0
		7	1.31	1.74	0.78	1.16	1.0
MSK			2.5	8	0.78	1.2	1.0

(2) Using the optimized efficient spectrum signal as the baseband modulation signal, the PAPR of the modulated signal after quadrature modulation is close to 1, with quasi-constant envelope characteristics. This shows that the purpose of reducing the PAPR of signals was achieved by introducing symbol-correlated characteristics and attenuation factor r.

(3) The attenuation at the first main lobe of the energy spectrum of the obtained signal is greater than 40 dB, while some attenuation is ≥ 70 dB (as shown in curve 3, Figure 3), which significantly reduced the out-band radiation of signals.

(4) The symbol length of the time-domain signal was increased, because of the introduction of intersymbol interference. However, because the two endpoints of the signals are smooth, the signal energy of the adjacent symbol is very small, proving that the introduction of intersymbol interference slightly affected the normal reception and decision of the signals.

4. Demodulation Scheme and Simulation Realization

4.1. Demodulation Scheme of System. The scheme of signal modulation is shown in Figure 2, and the coherent demodulation of signal can be achieved by the scheme shown in Figure 5.

The block diagram of coherent demodulation is shown in Figure 5, where t_a is the arrival time of the signal. The received modulated signal is coherently demodulated by the quadrature carriers and low-pass-filtered to remove the high-frequency components; it multiplied with a symbol envelope that delayed the corresponding times. Then, the two-channel signal was changed to a four-channel signal,

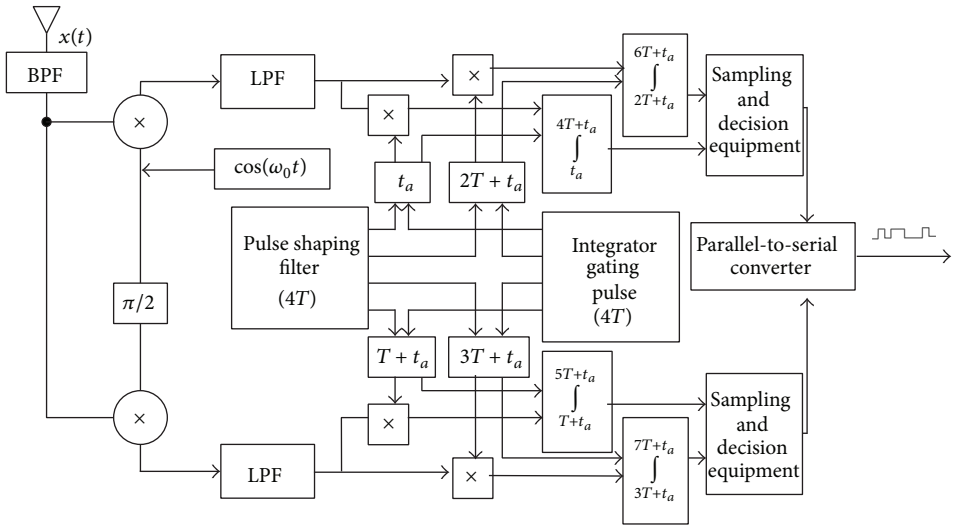

Figure 5: Block diagram of the coherent demodulation.

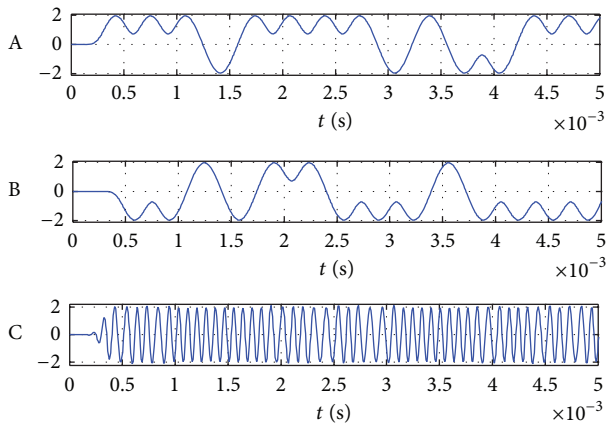

Figure 6: Simulation results of the quadrature modulation.

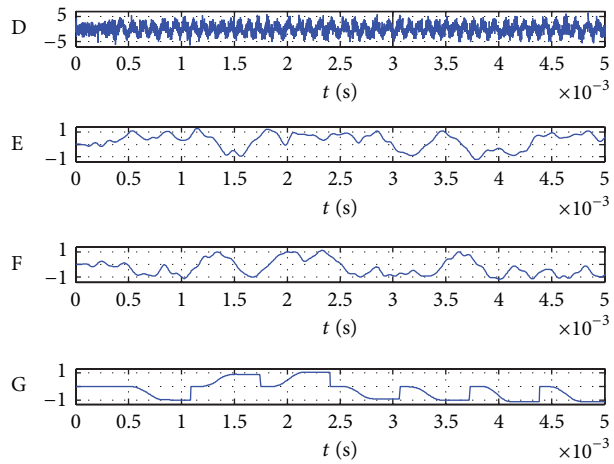

Figure 7: Simulation results of the coherent demodulation ($E_b/N_0 = 6$).

corresponding to the modulated signal on four channels. The signal on each channel was integrated (the integration time was controlled by the integrator strobe pulse). Finally, by sampling, decision, and a S/P converter, the four signal channels were combined into one signal channel; in this manner, the entire demodulation process was completed.

4.2. Simulation of Modulation and Demodulation. When $n = 3$, $m = 3$, and $r = 1$, the signal obtained was used as the baseband symbol, and the simulations of quadrature modulation and coherent demodulation were completed using the MATLAB software. The simulation results are shown in Figures 6 and 7.

In Figure 6, A is the baseband symbol signal transmitted in the in-phase channel, B is the baseband symbol signal transmitted in the orthogonal channel, and C is the quadrature-modulated output signal.

Figure 7 shows the simulation results of coherent demodulation when the E_b/N_0 is 6 dB. In Figure 7, D is the transmitted signal corrupted with additive white Gaussian noise (AWGN), which is the input to the receiver, E is the baseband signal demodulated in the in-phase channel, F is the baseband signal demodulated in the orthogonal channel, and G is the signal integrated by the integrator in Q channel. The sampling process was completed before the correlation integral of a symbol, which is before the arrival of integral reset pulse, and the transmitted data information was determined based on the sampling values.

The envelope of the output signal after the modulation was close to constant, consistent with the expected results. The simulation results of bit error rate (BER) for the E_b/N_0 is shown in Figure 8; the introduction of controlled intersymbol interference slightly affected the system's BER characteristics.

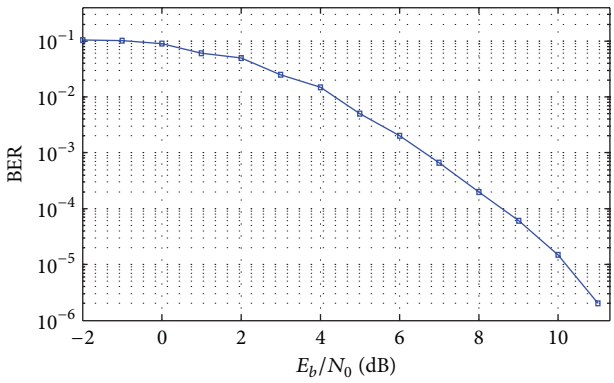

Figure 8: Bit error rate curves of simulation system.

5. Conclusions

In traditional communication modulation, the preexisting waveform is used as the baseband symbol signal, such as rectangular, cosine and raised cosine pulse, and other forms or through a filter (GMSK signal) to achieve frequency band compression. There are few uses of the method of establishing a mathematical model based on some standards to obtain the optimized baseband symbol signals. This paper proposes a method in accordance with the minimum out-band energy radiation criterion to establish a Pan-functional model for obtaining the optimized efficient spectrum signals. The calculation process was completed by introducing Fourier series and using the MATLAB software. Because of the introduction of controlled intersymbol interference and symbol-correlated characteristics, the obtained signals have the characteristics of a higher out-band spectral roll-off rate and quasi-constant envelope. Moreover, the spectral characteristics of the obtained signals are greatly superior to QPSK and MSK signals, even superior to the FQPSK signals in reducing the energy-band radiation and weakening the adjacent channel interference. Moreover, the introduction of the controlled intersymbol slightly affected the adjacent baseband symbol signal reception. The simulation of the signal modulation and demodulation scheme with controlled intersymbol interference was carried out using the MATLAB software. The simulation results show a constant-envelope carrier and continuous phase; thus, this method is feasible.

Conflict of Interests

The authors declare that there is no conflict of interests regarding the publication of this paper.

Acknowledgments

This research has been supported by International Science & Technology Cooperation Program of China (2014 DFR10240), China Postdoctoral Science Foundation (2013T60346), Harbin Science and Technology Research Projects (2013AE1BE003), and Heilongjiang Province Natural Science Foundation Projects (F201344). The authors are grateful to the editor and reviewers for their valuable comments.

References

[1] Z.-D. Xie, G.-X. Zhang, and D.-M. Bian, "A concatenated coded modulation scheme and its iterative receive for deep space communication," *Journal of Astronautics*, vol. 32, no. 8, pp. 1786–1792, 2011.

[2] K. S. Andrews, D. Divsalar, S. Dolinar, J. Hamkins, C. R. Jones, and F. Pollara, "The development of turbo and LDPC codes for deep-space applications," *Proceedings of the IEEE*, vol. 95, no. 11, pp. 2142–2156, 2007.

[3] C. Zhu and M. S. Corson, "A five-phase reservation protocol (fprp) for mobile ad hoc networks," *Wireless Networks*, vol. 7, no. 4, pp. 371–384, 2001.

[4] C. Liu, *Efficient Digital Modulation Technology and Its Application*, The People's Posts and Telecommunications Press, 2006.

[5] W. He, S. Du, and J. Yu, "Research into the technology of modulation and acquisition for cpm," *Electronic Science and Technology*, vol. 21, no. 3, pp. 38–42, 2008.

[6] Z. Cao and Y. Qian, *Modern Communication Theory*, The People's Posts and Telecommunications Press, 2006.

[7] K. Feher, *Wireless Digital Communications: Modulation and Spread Spectrum Applications*, Prentice-Hall PTR, Upper Saddle River, NJ, USA, 1995.

[8] H. Peng, J.-J. Wang, H.-F. Ding, and X. Yang, "An algorithm of OQPSK carrier synchronization based on quadratic spectrum," *Journal of Electronics and Information Technology*, vol. 33, no. 4, pp. 997–1001, 2011.

[9] X.-D. He, C.-X. Pei, and Y.-L. Meng, "A baseband GMSK signal correlator and its output probability distribution," *Journal of Electronics and Information Technology*, vol. 32, no. 10, pp. 2532–2535, 2009.

[10] Y.-C. Wu and T.-S. Ng, "Symbol timing recovery for GMSK modulation based on squaring algorithm," *IEEE Communications Letters*, vol. 5, no. 5, pp. 221–223, 2001.

[11] H. Zhao, D. Zhao, and C. Hou, "Design and implementation of msk modem," *Journal of Harbin University of Science and Technology*, vol. 16, no. 1, pp. 102–106, 2011.

[12] W. Zheng, "Parameter estimation of msk signals," *Journal of Circuits and System*, vol. 16, no. 2, pp. 23–27, 2011.

[13] L. Shkol'nyy, "The minimum out-of-band radiation optimization of radio pulse shape," *Radio Technology*, vol. 30, no. 6, pp. 12–15, 1975.

[14] W. Xue, W. Ma, and B. Chen, "A realization method of the optimized efficient spectrum signals using fourier series," in *Proceedings of the 6th International Conference on Wireless Communications, Networking and Mobile Computing (WiCOM '10)*, September 2010.

[15] Z. Dong, *Proficient in Programming and Database Applications of MATLAB7*, Publishing House of Electronics Industry, 2007.

[16] J. G. Proakis, *Digital Signal Processing: Principles Algorithms and Applications*, Pearson Education India, 2001.

[17] S. J. Mason and H. J. Zimmermann, *Electronic Circuits, Signals and Systems*, John Wiley & Sons, New York, NY, USA, 1960.

[18] H. Hu and R. Hu, *Calculus of Variations*, China Architecture and Building Press, 1987.

[19] L. Liu and J. Liang, "Clipping based mc-cdma system with lower peak-to-average power ratio," *Computer Engineering and Applications*, vol. 43, no. 22, pp. 129–132, 2007.

[20] J. Zheng, Q. Ying, and W. Yang, *Signals and Systems*, Higer Education Press, 2000.